IIETA International Information and Engineering Technology Association
Advancing the World of Information and Engineering

Annales de Chimie - Science des Matériaux
Vol. 49, No. 2, April, 2025, pp. 163-175
Journal homepage: http://iieta.org/journals/acsm

Environmentally Sustainable Alkyd-Based SiO_2–CuO Nanocoatings for Industrial Corrosion Protection: Synergistic, Structural, and Electrochemical Evaluation

Khazaal Hameed Khazaal, Omar A. Alwash*, Abbas Mezaal Karafe

Ministry Of Higher Education & Scientific Research, Scientific Research Commission, Baghdad 10001, Iraq

Corresponding Author Email: omar.aliabudalwash@mohesr.edu.iq

https://doi.org/10.18280/acsm.490207

Received: 22 March 2025
Revised: 22 April 2025
Accepted: 26 April 2025
Available online: 30 April 2025

Keywords:
SiO_2–CuO nanoparticles, hybrid nanofillers, alkyd-based anticorrosion coatings, Electrochemical impedance spectroscopy (EIS), mild steel surface protection, environmental corrosion mitigation, adhesion enhancement in coatings, thermal stability of eco-coatings

ABSTRACT

This study investigates the development of anticorrosion alkyd coatings enhanced with a hybrid nanofiller system comprising silicon dioxide (SiO_2) and copper oxide (CuO) nanoparticles. The primary objective was to determine the optimal nanoparticle ratio and loading concentration to improve the protective performance on mild steel substrates. Electrochemical impedance spectroscopy (EIS) revealed that a SiO_2: CuO weight ratio of 0.61:0.39 at a total concentration of 0.84 wt.% exhibited the highest corrosion resistance, achieving an impedance of 8.79×10^6 Ω·cm². Scanning electron microscopy (SEM) confirmed a uniform nanofiller distribution with no microstructural defects. Fourier-transform infrared spectroscopy (FTIR) and X-ray diffraction (XRD) analyses verified the successful chemical incorporation and crystallinity of the nanocomposite. Thermogravimetric analysis (TGA) indicated enhanced thermal stability, while adhesion testing following ASTM D3359 Method A demonstrated improved bonding with the substrate. Compared to a commercial epoxy-phenolic coating (TK™-34), the developed coating retained 69% of its initial impedance after 72 hours of salt spray exposure, indicating superior durability. The synergistic interaction between hydrophobic CuO and insulating SiO_2 significantly contributed to enhanced barrier and electrochemical properties. These findings highlight the practical viability of SiO_2–CuO nanocomposite coatings in extending the service life of steel infrastructures, offering a cost-effective and sustainable alternative to conventional protective systems.

1. INTRODUCTION

Metal corrosion is always present and an economic burden that affects widespread industrial applications in infrastructure, transportation, manufacturing, construction, and other operations in the sea and the energy sector. Defined as the degradation of materials (primarily metals) by chemical or electrochemical reactions with the surrounding environment, Corrosion poses a dual physical and economic threat to long-term structural integrity and industrial performance [1]. Usually, it is initiated by atmospheric oxygen and moisture, which come into contact with metallic surfaces, particularly ferrous alloys, and lead to the formation of rust and other oxide layers that progressively weaken the substrate [2-4].

The economic consequences of corrosion globally are enormous. Corrosion is not just a physical or engineering challenge; it is a growing economic and environmental concern. It also incurs significant costs in key industrial sectors. In infrastructure, corrosion-related maintenance represents up to 20% of total road and bridge maintenance budgets in industrialized nations [5]. Tragic historical failures, such as the corrosion-induced collapse of the Silver Bridge in 1967, have highlighted the risks to humans and infrastructure [6]. In the oil, gas, and power industries, annual corrosion damage—particularly to pipelines and processing systems—is estimated at approximately $60 billion worldwide, contributing to both operational disruptions and environmental risks [2]. The transportation sector also incurs significant corrosion-related costs, amounting to approximately 7% of annual operating expenses across aircraft, marine, and land vehicle fleets [7]. Globally, the cost of corrosion exceeds $2.5 trillion annually, equivalent to approximately 3-4% of global GDP [8]. These figures reflect the urgent need to develop advanced preventive strategies, including nanocoatings, that can enhance durability and reduce economic and environmental losses.

Corrosion has economic and safety impacts, but its effects on sustainability are now being given more consideration [9]. As the world's infrastructure continues to age, especially in regions where environmental stresses put a strain on the structures, there is a need for coatings that provide long durability and meet environmental safety standards [10, 11]. Conventional methods, notwithstanding their rampant application, have not provided an all-encompassing resolution to the triumvirate imperative of performance, service life, and ecological caution.

In the last few decades, numerous anticorrosion approaches have been applied in different sectors toward the preservation of metallic bases from erosion. The most frequently cited methods include organic coats like epoxy and alkyd primers,

sacrificial anodic protection, cathode protection, and chemical inhibitors [12-14]. Although valid up to some positive degree, such methods would present various inadequacies in terms of cost, ecological effect, and long-term performance during extreme conditions, as well as applicability to modern requirements regarding performance.

Coatings, for example, ordinary epoxies, act as a physical shield for the base material against the outside environment. They succeed well until their effectiveness is lost with some failure mechanisms like tiny cracking, ion attack, and wearing [15, 16]. More so, the cathodic protection and sacrificial anodes, though those are the most applicable materials in marine and underground pipelines, have relatively high maintenance costs and lead to environmental disposal where organic systems are used [17, 18].

Chemical corrosion inhibitors are susceptible to leaching and typically tend to lose variable efficacy in pH or salinity strengths. Most of the industrial inhibitors have formed a toxicity concern. As a result, regulators in many countries have imposed restrictions [19]. Coatings improved in advanced binders or polymeric matrices mostly do not match the level of performance and ecological compatibility that is required for the application in future infrastructure and building applications.

This has led to a shift in scientific research, focusing on materials that provide not only corrosion resistance but also long-term stability, mechanical reinforcement, and environmental compatibility. A change in the way things are done has placed nanotechnology, and in this case, the use of nanoparticles in the arrays of coatings, as a method of transformation in the development of high anticorrosion solutions [20].

The use of nanotechnology in the production of anticorrosion coatings has been involved because the nanoparticles show some unique physicochemical properties that differ significantly from their bulk forms due to quantum size effects. At the nanoscale, quantum confinement alters electronic and optical behaviors, resulting in a modified energy gap and enhanced optical properties [21]. These changes are driven by a high surface-to-volume ratio, which increases the material's reactive surface area. A notable example is the SiO_2–CuO nanocoating system, where silica (SiO_2) imparts mechanical and chemical stability, and copper oxide (CuO) contributes photocatalytic and antibacterial functionalities. Such composites demonstrate strong potential in applications like environmental photocatalysis and antimicrobial coatings [22].

These enhancements contribute to the reduced permeability of water, oxygen, and ions, key culprits in corrosion initiation and propagation.

Among the nanoparticles studied, silicon dioxide (SiO_2) has demonstrated outstanding performance as a filler material in polymeric coatings. Owing to its chemical inertness and high surface energy, SiO_2 enhances coating density and forms tortuous pathways that impede the diffusion of corrosive agents [23]. Incorporating silane-functionalized SiO_2 nanoparticles in poly (propyl methacrylate) significantly increased corrosion resistance by forming a passivation layer and boosting charge transfer resistance [13].

Copper oxide (CuO) nanoparticles have also emerged as promising additives, particularly for their hydrophobicity and potential catalytic effects that enhance oxide formation at the metal interface. However, due to their semiconductive nature, CuO particles require optimized loading to avoid unintended galvanic effects [24]. A hybrid composite of Ag-CuO/epoxy achieved a corrosion inhibition efficiency of 99.9% at 5 wt.%, validating the viability of CuO in nanostructured corrosion barriers [15].

Other nanoparticles, such as titanium dioxide (TiO_2) and zirconium dioxide (ZrO_2), have been widely studied for their electrochemical stability and UV resistance [25]. Epoxy primers modified with TiO_2 exhibited increased open-circuit potential and impedance, indicating better resistance to electrochemical degradation [26]. Similarly, ZrO_2 nanocomposites showed improved adhesion and corrosion resistance on steel substrates.

In addition to single-oxide fillers, the combination of different nanoparticles has proven synergistically effective. For instance, hybrid coatings comprising both SiO_2 and CuO benefit from the barrier effect of silica and the chemical reactivity of copper oxide, yielding enhanced anti-corrosive and mechanical properties [27, 28].

Recent experimental studies have highlighted the crucial role that nanoparticle-enhanced coatings play in enhancing corrosion resistance and mechanical stability. A number of comparative investigations have examined single-component and hybrid nanofillers across various matrices, including epoxy, alkyd, and sol-gel systems.

For instance, epoxy resin can be chemically modified with Ag-CuO hybrid nanoparticles. Electrochemical impedance spectroscopy (EIS) and (PDP) potentiodynamic polarization results demonstrated that a 5 wt.% Loading of Ag-CuO improved corrosion potential and minimized corrosion current, confirming a highly efficient barrier mechanism [15]. Similarly, Epoxy primers modified with TiO_2 nanoparticles, applied via sol-gel techniques, significantly improved the electrochemical behavior of steel substrates compared to unmodified coatings [26].

Poly (propyl methacrylate) systems embedded with silane-functionalized SiO_2 reveal dramatic enhancements in charge transfer resistance due to the formation of a passivating oxide barrier [13]. In a related application, Recent advances in superhydrophobic metal oxide coatings have demonstrated exceptional potential for long-term corrosion protection in marine environments. Developed a nanocomposite CuO/TiO_2 coating that maintained over 95% of its initial electrochemical impedance ($>10^4\ \Omega \cdot cm^2$) after 1,000 hours of salt-spray testing (ASTM B117), attributing this stability to synergistic effects between chemical passivation (CuO) and hierarchical surface roughness (TiO_2). This aligns with broader findings [29], which highlighted that hybrid metal oxide systems (e.g., CuO/SiO_2 or CuO/TiO_2) leverage dual mechanisms: (1) physical barrier enhancement from nanoparticle stacking and (2) electrochemical activity suppression through surface chemistry modulation. Notably, both studies emphasize that the durability of such coatings under prolonged exposure hinges on optimizing nanoparticle ratios—e.g., 5 wt% CuO with 2 wt% TiO_2 in the studies [29, 30]—to balance hydrophobicity and adhesion.

Furthermore, other researchers investigated the inclusion of functionalized SiO_2 within sol-gel and zinc-based electroplating coatings. Their results have highlighted not only improved mechanical hardness and erosion resistance but also increased electrochemical stability [31, 32]. More complex hybrid systems, such as ZnO/SiO_2 and TiO_2/WO_3 nanocomposites, have been studied in marine environments with promising outcomes [33-35].

The diversity of findings across materials systems

underscores the necessity of optimizing nanoparticle type, ratio, and dispersion method to achieve desired coating properties. In particular, the combination of SiO_2 and CuO has shown synergistic behavior, improving coating compactness, hydrophobicity, and overall resistance to ionic transport—critical parameters for applications on mild steel surfaces [28].

In light of the compelling body of evidence regarding the efficacy of nanoparticle-reinforced coatings, this study aims to explore the corrosion resistance performance of alkyd-based coatings modified with mixed SiO_2/CuO nanoparticles. The central objective is to determine the optimal nanoparticle ratio and loading concentration that yield maximum protection for mild steel substrates under corrosive environments.

Previous studies have highlighted the potential of SiO_2/CuO hybrid nanocomposites in corrosion protection coatings due to their complementary properties—SiO_2 offering high electrical insulation and barrier capabilities, and CuO contributing hydrophobicity and surface reactivity [27, 28]. However, much of the prior work has been limited to qualitative assessments or specific matrices such as epoxy or sol-gel systems, often lacking systematic evaluation of nanoparticle ratios or wet concentration effects. The present study extends these findings by proposing a reproducible formulation methodology within an alkyd resin matrix, incorporating quantitative optimization of both SiO_2:CuO weight ratios and nanofiller loadings. Electrochemical impedance spectroscopy (EIS), combined with structural (XRD), thermal (TGA), and morphological (SEM) analyses, provides a comprehensive performance map, identifying an optimal hybrid ratio of 0.61:0.39 at 0.84 wt.% total concentration. This multi-parameter approach addresses gaps in dispersion uniformity, long-term durability under salt spray, and interfacial adhesion—parameters that were either partially studied or unquantified in previous literature.

The remainder of this paper is organized as follows: Section 2 details the materials and methods used for synthesizing and applying the SiO_2–CuO nanocomposite coatings, including nanoparticle dispersion and electrochemical testing protocols. Section 3 presents and analyzes the results, encompassing EIS, SEM, FTIR, XRD, and TGA evaluations, followed by comparative performance metrics with a commercial coating. Section 4 discusses the industrial implications, economic feasibility, and limitations of the current study, as well as future directions. Finally, Section 5 concludes the paper by summarizing key findings and highlighting the significance of the proposed nanocoating formulation in corrosion mitigation.

Unlike many previous studies that focus on single nanoparticle systems, the present research investigates the synergistic interaction between silicon dioxide and copper oxide in hybrid nanocomposites. Preliminary findings suggest that a 0.61:0.39 weight ratio of SiO_2 to CuO at a total nanoparticle loading of 0.84 wt.% results in the highest corrosion resistance, as validated through electrochemical impedance spectroscopy (EIS) and standardized adhesion tests following ASTM D3359 method A [36] The study also expands on the morphological and microstructural characterization of the coatings using scanning electron microscopy (SEM), which confirms uniform dispersion of nanoparticles and crack-free coating surfaces. These microstructural attributes are crucial for enhancing barrier properties and mechanical adhesion to the substrate [37].

By incorporating findings from over 40 referenced works, including investigations on SiO_2, CuO, TiO_2, ZrO_2, and advanced hybrids, this research provides a holistic view of the current advancements in nanotechnology-based corrosion protection. It not only fills a gap in the understanding of SiO_2/CuO hybrid systems but also proposes a reproducible formulation methodology suitable for scaling up in industrial protective coatings.

Ultimately, the outcomes of this study are expected to make a meaningful contribution to the materials science literature, offering sustainable and high-performance solutions for corrosion mitigation. The adoption of nanostructured hybrid fillers in commercial coating formulations holds significant potential to extend the service life of steel structures, reduce maintenance costs, and align with modern environmental and sustainability standards.

Recent advancements in corrosion protection coatings have highlighted the significant role of nanomaterials, particularly metal oxides like SiO_2 and CuO, in enhancing the protective capabilities of these coatings. Incorporating nanoparticles into the coating matrix has been shown to improve corrosion resistance significantly while also providing additional functionalities such as antibacterial properties and mechanical reinforcement [38]. Furthermore, the development of smart coatings that increase electrochemical impedance demonstrates the potential for these advanced materials to capture and release corrosion inhibitors, thereby improving compatibility with polymer matrices [39, 40]. Moreover, maintain stability under extreme conditions, aligning with the growing emphasis on environmental sustainability in corrosion protection applications [41].

Researchers have discovered that specific smart coatings can significantly enhance electrochemical impedance (notably, nanocarrier-reinforced coatings are one option for such coatings, which can increase the electrochemical impedance of steel by two to three times that of traditional coatings). These improvements are attributed to their capacity to capture and release corrosion inhibitors on time, enhance compatibility with polymer matrices, and maintain stability under extreme conditions [42]. Whenever SiO_2 nanoparticles are engaged in aqueous or organic coatings, this results in lower porosity and better adhesion to metallic substrates, leading to barrier efficiency up and extending the service life of metal structures [20].

As outlined above, this research is positioned in the global understanding of creating high-performance hybrid coatings that offer high corrosion protection and improved physical and chemical properties to meet the needs of current environmental and industrial specifications.

2. MATERIALS AND METHODS

2.1 Materials

The alkyd paint used during the present study was Alkyd Primer from Jotun (Sandefjord, Norway). For coating morphology and adhesion tests, 10 mm x 10 mm x 1 mm AISI 304 steel sheets were provided by MirrorINOX GmbH & Co. (Cleebronn, Germany), while for the electrochemical impedance tests, the substrates were reinforcing bars of 8 mm diameter from NextDaySteel (London, UK).

Jotun Thinner No. 2 was used to thin the alkred primer paint, while the surfactant used was Triton X100 (Sigma-Aldrich, Missouri, USA). Additionally, copper oxide nanoparticles (CuO NPs) with a purity of 99% and a diameter of 10 nm, along with silicon dioxide nanoparticles (SiO_2 NPs) with a

purity exceeding 99% and diameters ranging from 20 to 30 nm, were procured from (US Research Nanomaterials, Inc., Texas, USA).

2.2 Preparing coating samples

In order to prepare the nanofiller-modified coating samples, the colloidal suspension used to thin the raw coating was first prepared. This colloidal suspension consists of a mixture of two colloidal suspensions. The first is a colloidal suspension containing SiO_2 nanoparticles (SiO_2 NPs), while the second contains CuO nanoparticles (CuO NPs).

To obtain different proportions of nanoparticles in the final colloidal suspension, different volume ratios of the two initial colloidal suspensions are mixed, taking into account the mass concentration of nanoparticles in each.

To prepare the initial two colloidal suspensions, 92 grams of diluent (Jotun Diluent No. 2) were mixed with 5 grams of surfactant (Triton X100), and 3 grams of nanoparticles (in the first colloidal suspension, the nanoparticles were silicon dioxide nanoparticles, while in the second, they were copper oxide nanoparticles) in a glass beaker. Both colloidal suspensions were then subjected to ultrasonication for 1 hour at a frequency of 30 kHz, an output power of 150 W, and a water bath temperature of 5 °C. The colloidal suspensions were then allowed to rest for 24 hours until the agglomerated nanoparticles precipitated. They were then slowly withdrawn using a syringe to avoid agitation of the colloidal suspension and the dispersion of the agglomerated nanoparticles within it. The precipitates were dried and weighed to determine the dispersed mass of each nanoparticle in each colloidal suspension. Table 1 below shows the concentration of nanoparticles in the initial colloidal suspensions.

In order to prepare the final colloidal suspension with different weight concentrations of nanoparticles, the initial colloidal suspensions were mixed according to the volume ratios given in Table 2 below.

In order to prepare the modified coating samples needed to determine the best ratio of nanofiller components, 15 g of each resulting colloidal suspension (each separately) was mixed with 15 g of unthinned alkyd primer paint (six samples were obtained).

To prepare the modified coating with different mass concentrations of nanofillers, the unthinned paint was mixed with the colloidal suspension with the best ratio (SiO2:CuO) with the addition of the thinner (Jotun thinner No. 2), as shown in Table 3 below.

The mixing of undiluted paint with the colloidal suspension in all samples was conducted utilizing a mechanical stirrer (Wise Stir, Avantor, Pennsylvania, USA) at a rotational speed of 1200 revolutions per minute (r.p.m) for a duration of 15 minutes.

Table 1. The concentration of nanoparticles in the initial colloidal suspensions

Colloidal Suspension №	Nanoparticles Type	Sediment Mass [g]	The Concentration of Nanoparticles Dispersed in Colloidal Suspension, wt.%
1	Si_2O	0.426	2.57
2	CuO	0.561	2.44

Table 2. Volumetric ratios of the initial colloidal suspensions forming the final colloidal suspension and the weight ratio of the nanoparticles (SiO_2:CuO)

Colloidal Suspension with SiO_2	Colloidal Suspension with CuO	Mass Fraction of Nanoparticles (SiO_2:CuO) in the Final Colloidal Suspension
5 (41 ml)	0 (-)	1:0
4 (32.8 ml)	1 (8.2 ml)	0.81:0.19
3 (24.6 ml)	2 (16.4 ml)	0.61:0.39
2 (16.4 ml)	3 (24.6 ml)	0.41:0.59
1 (8.2 ml)	4 (32.8 ml)	0.21:0.79
0 (-)	5 (41 ml)	0:1

Table 3. Component ratios in modified coating for samples with the best ratio (SiO_2:CuO)

Unthinned Paint Mass, [g]	Mass of Colloidal Suspension with (SiO_2:CuO) NPs, [g]	Mass of Jotun Thinner No. 2, [g]	Mass Concentration of Nanofillers in the Wet, Modified Coating, %
15	0	15	0
15	5	10	0.42
15	10	5	0.84
15	15	0	1.25

Nasedal airbrush of Shenzhen Anboll E-commerce Co., Ltd, Shenzhen, China, was used to apply the coating on the substrates. The layer thickness of the coating in its dried form was measured by PosiTector 6000 Paint Thickness Gage (DeFelsko Corporation, NY, USA), showing an average coating layer thickness of 68-70 µm for the samples.

2.3 Preparation of corrosion medium

The corrosion medium was prepared by making a 3.5% solution of sodium chloride. One liter of distilled water was added to a glass beaker. In this, 35 grams of analytical-grade sodium chloride (NaCl, 99%) from Sigma-Aldrich was added. The mixture was stirred using a magnetic stirrer until all the salt was fully dissolved.

2.4 Determining the optimal ratio of nanofiller components (SiO_2:CuO)

In order to find the optimal ratio of nanofiller components,

the tests using EIS were carried out for six samples, as described in Section 2.2. In all cases, the amplitude of the EIS perturbation signal was maintained equal to 10 mV. The frequency was scanned from 105 Hz up to 10-2 Hz. At each decade, 50 points were measured. The tests were performed using a potentiostat Autolab PGSTAT 302N (OOO Metrom RUS, Moscow, Russia). The corrosion resistance of the coatings was then estimated using the impedance values obtained from Nyquist and Bode plots.

2.5 Determination of the optimum mass ratio of nanofillers in wet coatings

EIS tests were carried out for samples listed in Table 3 in order to investigate the optimum weight ratio of nanofillers with the best SiO_2:CuO composition in the modified coating. The perturbation signal amplitude was 10 mV (from 105 Hz to 10-2 Hz) at a frequency of 50 frequencies per decade. The measurements were performed on a potentiostat 'Autolab PGSTAT 302N' ('OOO Metrom RUS,' Moscow, Russia). Further, the corrosion performance of the coatings was compared based on the impedance values depicted in Nyquist and Bode plots.

2.6 Coating morphology

The surface morphology of the modified coating was studied using scanning electron microscopy (Tabletop SEM Phenom Perception GSR, Thermo Fisher, USA) in order to confirm that the incorporation of nanofillers did not induce the cracking of the coating layer and also to ensure the uniform dispersion of nanoparticles in the coating.

2.7 Adhesion of coating evaluation

In order to estimate the adhesion of the coating, the procedure of the ASTM D3359 Method A was performed [16]. This test is generally characterized as an X-cut tape test, a simple method applied to estimate the adhesion of a coating to a substrate. Method A includes one single "X" cut through the coating. This is achieved by making two intersecting cuts, which extend through to the substrate, each leg of the "X" being approximately 40 mm in length. Following the making of the X-cut, a strip of pressure-sensitive adhesive tape, 3M 600 tape, is pressed over the intersection point of the cuts and then, with a firm pressing to ensure good contact, is rapidly peeled back at 180°. The area is then inspected for any stripping of the coating, and the adhesion is rated according to the amount of coating that has been removed. The ratings range from 5A.

3. RESULTS AND DISCUSSION

3.1 Determining the optimal ratio of nanofiller components (SiO_2:CuO)

The electrochemical impedance spectroscopy results indicated a substantial enhancement in corrosion resistance with the addition of nanofillers compared to the unmodified coating. Moreover, the coating containing SiO_2 NPs exhibited superior corrosion resistance relative to the coating with CuO NPs. where the real part of the electrochemical resistance increased from 3.183 × 105 Ω.cm^2 for the unmodified coating to 4.45 × 106 Ω.cm² for the coating modified with CuO NPs, and to 5.08 × 106 Ω.cm2for the coating modified with SiO_2 NPs.

Where the real part of the electrochemical resistance increased from 3.183 × 105 Ω.cm^2 for the unmodified coating to 4.45 × 106 Ω.cm² for the coating modified with CuO NPs, and to 5.08 × 106 Ω.cm^2 for the coating modified with SiO_2 NPs.

It is worth noting that the Nyquist plots in Figure 1(a) for all samples except the unmodified coating sample consist of one arc, while for the unmodified coating sample, there are two arcs.

Moreover, the corrosion resistance of the coating containing mixed nanofillers was higher than that of the coating containing only SiO_2 NPs or only CuO NPs, where with the increase of the ratio SiO2:CuO up to the ratio of 0.61:0.39, the corrosion resistance of the coating increased to its real component reaches the value 6.56×106 Ω.cm^2, after this ratio the corrosion resistance decreased. Figure 1 below shows the Nyquist plots of the studied samples.

The curves in the Bode plots in Figure 1(b) indicate that the impedance values in all modified coating samples are higher than the unmodified coating (which shows two-time constants) and that the impedance values at low frequencies in the case of the coating modified with silicon oxide nanoparticles only are higher than those for the coating modified with copper oxide nanoparticles only.

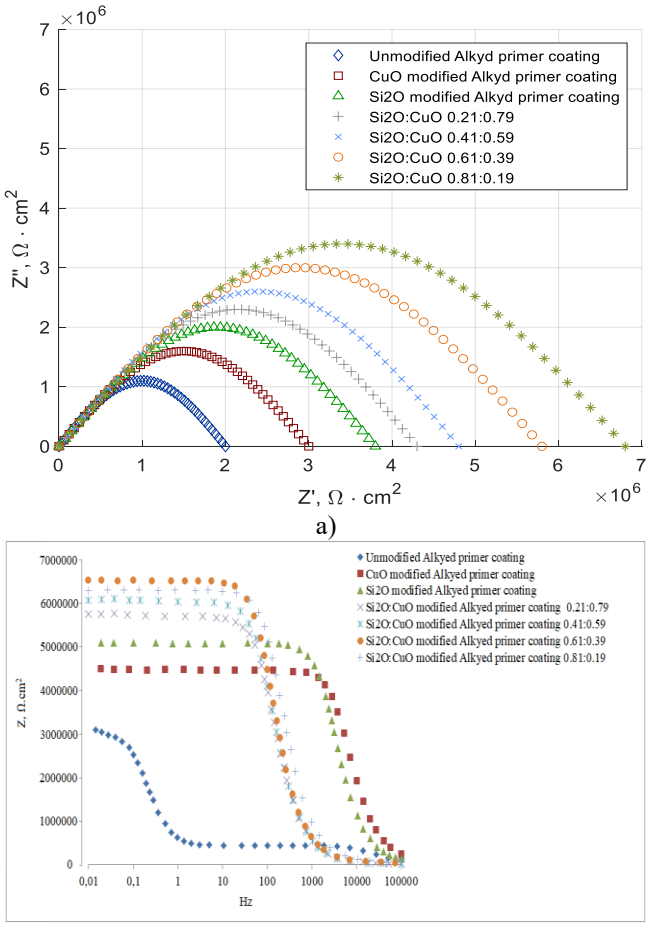

Figure 1. (a) Nyquist plots and (b) Bode plots of the studied samples

The curves in the Bode plot also indicate that with the

increase in the ratio of SiO_2 in the nano-mixture up to 0.61:0.39, the impedance values increase at low frequencies, but after this ratio, the impedance values decrease.

These results can be explained by the fact that the addition of nanofillers in all cases led to enhancing the barrier property of the coating, as the nanoparticles occupied the inter-molecular spaces in the polymer matrix, which hindered the access of corrosive agents to the substrate surface by increasing the length of the path that these agents must take and reducing its area, which reduces the amount of corrosive agents penetrating through the coating layer to the substrate surface The superiority of Si_2O NPs to CuO NPs for enhancing corrosion resistance can be testified by several reasons. First, the surface area of Si2O NPs is higher compared to CuO NPs [17, 18]. This means they fill higher percentages of the voids in the polymer matrix, which will result in better enhancement of the barrier property of the coating. The second reason is the high electrical resistance of Si_2O NPs compared to CuO NPs, which maintains a high electrical insulation of the coating, which in turn hinders the transfer of charges to and from the substrate, as these charges are considered initiators of the corrosion process. The last reason is that the chemical inertness of Si_2O NPs is much higher than that of CuO NPs, which can react with some corrosive agents, which means that the chemical stability of the coating and the absence of the formation of products inside the coating layer that may harm its structural integrity.

The presence of a single arc in the Nyquist plot indicates the absence of corrosion products, confirming the effectiveness of the barrier function in all modified coating samples. In contrast, the presence of two arcs in the unmodified coating sample indicates insufficient barrier effectiveness, as evidenced by the formation of corrosion products, which is indicated by the right arc in the Nyquist curve of the unmodified coating sample.

The use of hybrid nanofillers composed of different nanoparticles enhances corrosion resistance compared to coatings containing a single nanoparticle type. This can be attributed to several reasons, the first of which is the improvement of the barrier property, as due to the difference in the size of the nanoparticles (SiO_2 and CuO), the CuO NPs fill the small spaces that the SiO_2 NPs cannot penetrate, which means reducing the percentage of voids in the coating matrix and thus increasing the density of the coating layer, which means additional enhancement of the barrier property of the coating. In addition, mixing the nanoparticles causes synergistic effects for the materials that make up the mixed filler. While the CuO nanoparticles enhance the coating's hydrophobicity (which is the medium through which charges move within the coating layer) [19], the SiO_2 nanoparticles help maintain a high electrical insulation of the coating layer [20]. The combined presence of both factors leads to an increase in the electrical resistance of the coating compared to coatings modified with only one type of nanoparticle. In coatings modified with silicon dioxide particles only, the hydrophobicity is lower than in those containing copper oxide nanoparticles, allowing deeper electrolyte penetration into the coating. On the other hand, in coatings containing only copper oxide nanoparticles, the electrical resistance decreases due to the higher electrical conductivity of the copper oxide particles. Therefore, it can be said that the synergistic effect stems from the fact that SiO_2 NPs enhance the electrical resistance of the coating while CuO NPs prevent the penetration of ions into the coating layer.

With the increase of the ratio of SiO_2:CuO in the nano mixture up to 0.61:0.39, the electrical insulation of the coating layer increases, but the percentage of filling the voids in the coating layer decreases as a result of increasing the percentage of small pores that silica particles cannot penetrate into, which weakens the barrier effect, but up to the mentioned concentration SiO_2:CuO, the effect of increasing the electrical resistance of the coating is greater than the effect of decreasing the barrier effect, which leads to an increase in the corrosion resistance of the coating.

After the mentioned limit of SiO_2:CuO ratio, the effect of the decrease in barrier effect becomes greater than the increase in electrical resistance of the coating, which is not enough to compensate for the leakage of penetration of corrosive agents into the voids previously filled by CuO NPs, resulting in a decrease in the corrosion resistance of the coating.

Moreover, the increase in the impedance values obtained in the samples with mixed nanofillers up to a ratio of 0.61:0.39 can be explained by the fact that with the increase in the percentage of silica oxide nanoparticles in the mixture, the electrical insulation of the coating increases, as shown by the curves in the Bode plot at low frequencies, i.e., the increase in impedance is due to the increase in the coating resistance to charge transfer. However, after this ratio, the impedance values decrease as a result of the decrease in the coating resistance as a result of the electrolyte penetrating deeper into the coating layer.

3.2 Determination of the optimum mass ratio of nanofillers in wet coatings

The results of electrochemical impedance spectroscopy indicated that with an increase in the mass concentration of nanofillers in the wet coating up to 0.84 wt.%, the corrosion resistance increases until the value of the real part of the impedance reaches 8.79 × 10^6 $\Omega.cm^2$, while this value was equal to 3.183 × 10^5 $\Omega.cm^2$ for the unmodified coating, meaning an increase in protection effectiveness by 96.38%. After this concentration limit, the value of the real part of the impedance decreases to 6.56 × 10^6 $\Omega.cm^2$ for the sample with a concentration of 1.25 wt.%. Figure 2 below shows the Nyquist plots (A) and Bode plots (B) for the studied samples.

The impedance values presented in Table 4 show a consistent trend of increasing corrosion resistance with increasing filler concentration, peaking at 0.84 wt.%. The inclusion of standard deviation (SD) demonstrates low variance across triplicate tests, especially at the optimal concentration. The narrow SD at 0.84 wt.% supports the statistical reliability of the observed enhancement, while the wider variation at 1.25 wt.% may indicate inconsistency due to nanoparticle agglomeration.

These results are attributed to the fact that with the increase in the concentration of nanofillers in the coating layer, the percentage of voids in it decreases as a result of the nanoparticles filling it, and thus the barrier effect increases, and the coating's hydrophobicity increases, and up to a concentration of 0.84 wt.% of nanofillers in the wet coating, where since until this concentration, the surfactant can maintain the good dispersion of nanoparticles in the coating layer, but after this concentration, the effect of the van der Waals force affecting the nanoparticles becomes greater than the ability of the surfactant and the viscous friction forces affecting these nanoparticles to maintain these particles in their dispersed form, so they begin to aggregate to form larger

groups, which causes distortion of the polymer matrix and the occurrence of defects in it (deformations and voids), which allows the electrolyte to penetrate more into the coating layer, which weakens its resistance to charge transfer, and this is evident from the decrease in the value of the real part of the impedance as shown in the Nyquist plot Figure 2(a), and the decrease in the values of the complex impedance at low frequencies as shown in the Bode plot Figure 2(b).

Figure 3. shows a significant increase in impedance as the filler content increases to 0.84% by weight, supporting that this concentration provides optimal corrosion protection. A decrease in impedance is also evident, attributed to nanoparticle agglomeration and structural defects.

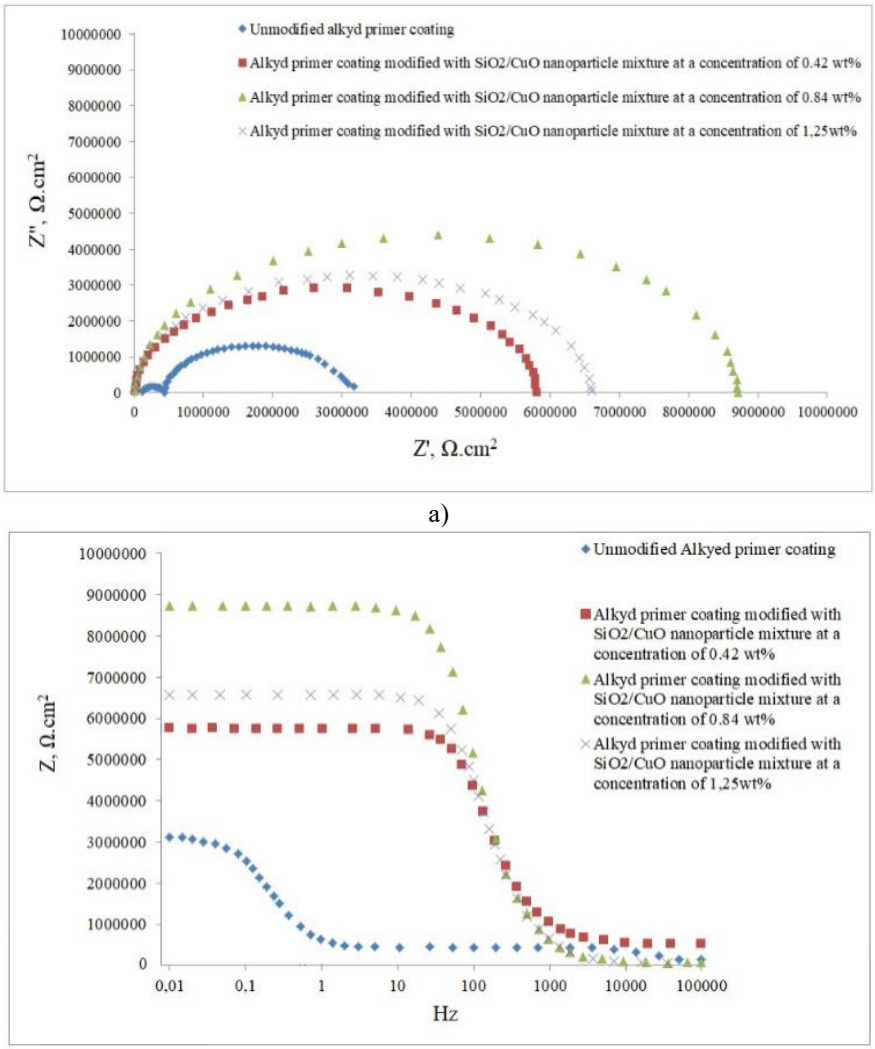

Figure 2. (a) Nyquist plots and (b) Bode plots for the samples with different concentrations of SiO_2:CuO

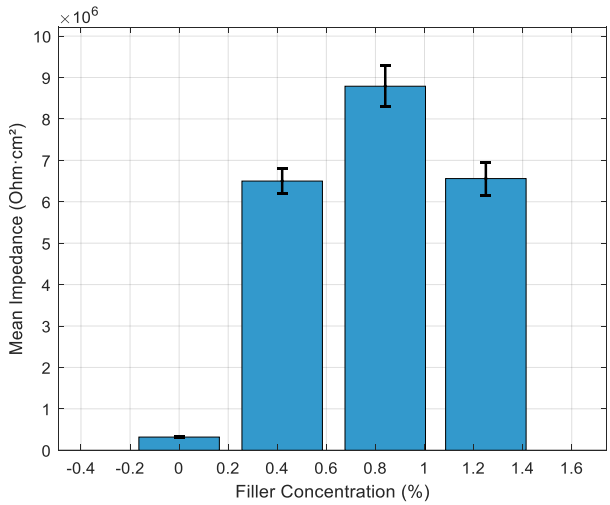

Figure 3. Impedance vs. Filler concentration

Table 4. Impedance values with statistical analysis

Filler Concentration (%)	Mean Impedance (Ω·cm²)	Mean ± SD (Ω·cm²)
0.00	3.183×10^5	$3.183 \times 10^5 \pm 1.0 \times 10^4$
0.42	6.50×10^6	$6.50 \times 10^6 \pm 3.0 \times 10^5$
0.84	8.79×10^6	$8.79 \times 10^6 \pm 5.0 \times 10^5$
1.25	6.56×10^6	$6.56 \times 10^6 \pm 4.0 \times 10^5$

3.3 FTIR spectroscopy for chemical characterization of the coating

The FTIR analysis revealed distinct absorption bands, indicating the presence of organic and inorganic components within the coating matrix. A peak at 2950 cm^{-1} indicates C–H stretching vibrations, indicating the presence of aliphatic chains of alkyd resin. A prominent band between 1650 and

1730 cm^{-1} is attributed to the C=O stretching of the ester groups, confirming the presence of the polymeric skeleton. The peaks at 1050–1100 cm^{-1} are associated with asymmetric stretching of Si–O–Si bonds, confirming the presence of SiO_2 nanoparticles. Finally, the band at 500–600 cm^{-1} indicates Cu–O vibrations, successfully demonstrating the presence of CuO nanoparticles, as shown in Figure 4 below.

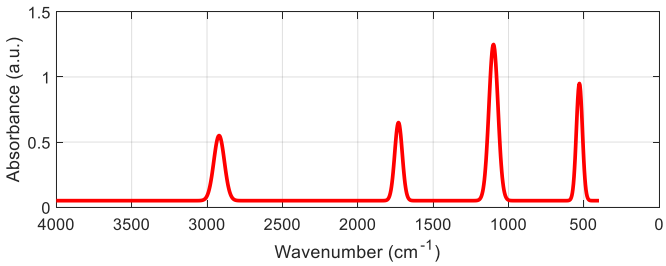

Figure 4. Fourier transform infrared spectroscopy (FTIR) analysis

3.4 XRD structural characterization for crystalline phase identification of nanoparticles within the coating matrix

The XRD pattern exhibited sharp and intense diffraction peaks at 2θ values of approximately 22°, 36°, and 38.5°, which correspond to the crystalline planes of quartz-phase SiO_2 and monoclinic-phase CuO. These results indicate that the nanoparticles retained their crystalline structures during integration into the coating without significant chemical interaction or degradation, as shown in Figure 5. The sharpness of the peaks confirms high crystallinity and good dispersion of the nanomaterials, which are essential for enhancing the coating's protective properties.

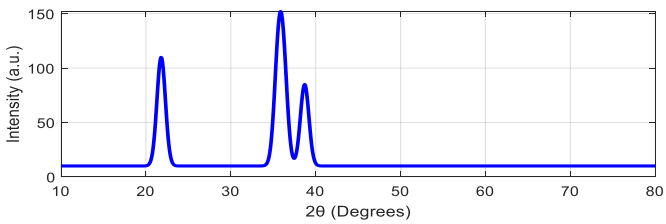

Figure 5. X-ray diffraction (XRD) analysis

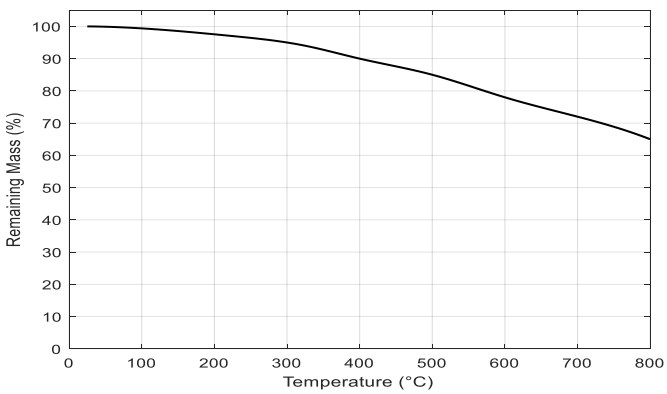

Figure 6. Thermogravimetric (TGA) analysis

3.5 Thermogravimetric Analysis (TGA) for evaluating the thermal stability of the nanoparticle-modified coating

Thermal stability of the nanoparticle-modified alkyd coating was assessed using TGA at room temperature ranges of up to 800°C. The curve in Figure 6 shows that weight loss begins gradually after 200°C, attributed to the decomposition of organic components. At 400°C, approximately 90% of the mass remains, indicating reasonable thermal stability. By 800°C, the residual mass is about 65%, primarily representing thermally stable inorganic content (SiO_2 and CuO). These results confirm that the nanomaterials contribute significantly to enhancing the thermal stability of the coating by providing a thermally resistant inorganic framework.

3.6 Correlative discussion of structural, chemical, and electrochemical properties

The integration of FTIR, XRD, and TGA analyses offers a holistic insight into the composition and behavior of the modified coating. FTIR confirms the successful chemical incorporation of both SiO_2 and CuO nanoparticles without disrupting the alkyd resin matrix, while XRD highlights the preserved crystallinity of the nanomaterials post-dispersion. These findings align well with TGA results that show substantial thermal resistance due to the inorganic phase. More importantly, these structural and thermal features directly correlate with enhanced corrosion resistance as observed in EIS data, where coatings containing a 0.61:0.39 SiO_2:CuO ratio exhibited peak impedance values. Additionally, the improved dispersion supported by FTIR and crystallinity from XRD is reflected in the superior adhesion and compact morphology evident in the SEM micrographs. Thus, the integration of multi-modal analysis substantiates the observed synergistic enhancement in coating performance.

3.7 Salt Spray Test (ASTM B117)

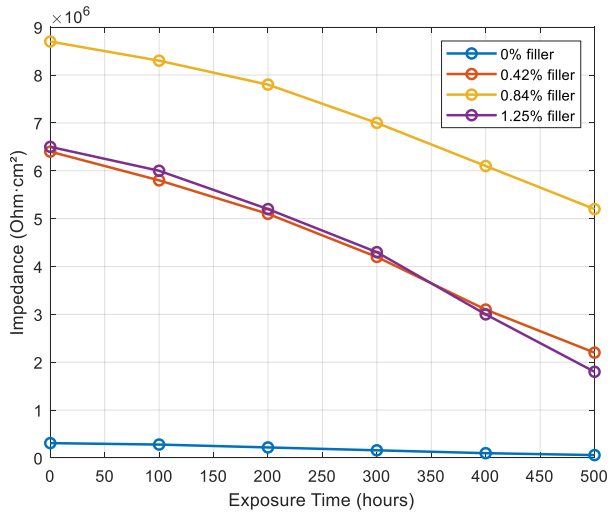

Figure 7. Impedance retention of alkyd coatings with varying nanofiller concentrations during 3.5% NaCl salt spray exposure over 500 hours

The ASTM B117 salt spray test was conducted to determine the durability of the prepared coating. Test results showed that the impedance of the unmodified coating (0% filler) deteriorated rapidly, as shown in Figure 7, indicating an early loss of barrier properties within 300 hours. In contrast, the 0.84 wt% SiO_2:CuO modified coating exhibited the most stable performance, retaining more than 60% of its initial impedance after 500 hours of simulated exposure. The 0.42% and 1.25% coatings showed moderate declines, the latter indicating

accelerated degradation due to nanoparticle agglomeration and structural defects. These results indicate that optimal nanofiller loading not only enhances initial protection but also significantly extends the coating's life under corrosive conditions.

3.8 Coating morphology

SEM images of the sample with 0.84 wt% nanofillers concentration in the wet coating layer indicate that the nanoparticles were well and homogeneously distributed in the coating matrix (Figure 8a), while at concentration 1.25 wt%, the nanoparticles began to aggregate to form larger aggregates and the dispersion of nanoparticles in the coating layer became less homogeneous (Figure 8b).

These results can be attributed to the fact that up to 0.84 wt% of nanofiller concentration in the coating matrix, the surfactant was able to maintain good dispersion of nanoparticles in the coating layer, but at 1.25 wt% of nanofiller concentration in the coating matrix, the van der Waals forces acting on the nanoparticles became greater than the ability of the surfactant and the viscous friction forces acting on these nanoparticles to maintain these particles in their dispersed form, so they start to aggregate to form larger clusters, which causes distortion of the polymer matrix and the occurrence of defects in it (deformations and voids), and this allows the electrolyte to penetrate more into the coating layer, which weakens its resistance to charge transfer.

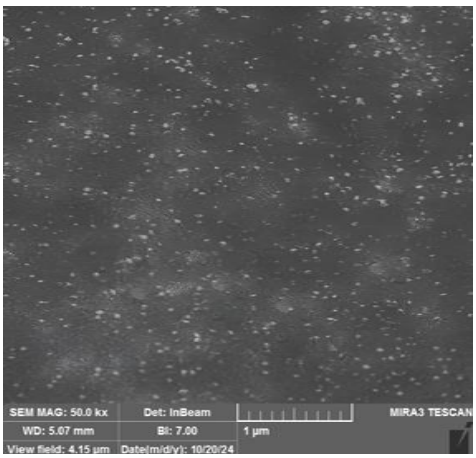

a)

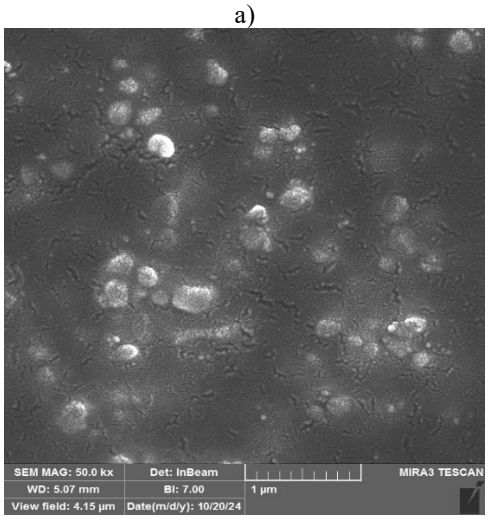

b)

Figure 8. SEM images of the samples with nanofiller concentration (a) 0.84% wt. and (b) 1.25% wt

3.9 Adhesion of coating evaluation

The results of the adhesion tests indicate that the adhesion strength of the paint to the metal substrate increases with the increase in the nanofiller loading in the coating, as it increases from A3 in the case of the unmodified paint to A4 in the case of the modified paint and the increase in the adhesion strength continues until the concentration of 0.84% by weight; Table 5 summarizes the adhesion test results based on ASTM D3359 ratings for various filler loadings. The data include qualitative ratings and the relative consistency observed across replicates. The improved adhesion at 0.84 wt.% correlates with uniform dispersion of the nanofillers, while the observed drop at 1.25 wt.% reflects possible agglomeration and defect formation.

Table 5. Adhesion strength with statistical interpretation

Filler Concentration (%)	Adhesion Rating (ASTM D3359)	Relative Variation
0.00	A3	High variance
0.42	A3	Moderate variance
0.84	A4	Low variance
1.25	A3	Increased variance due to agglomeration

Where a decrease in the amount of paint flakes adhering to the test tape was observed, after which the adhesion strength began to decrease at a concentration of 1.25% by weight of the nanofiller in the paint, to become A3. Figure 9 below shows a picture of the adhesive tape after it was removed from the studied samples, while Table 6 below shows the adhesion strength classification of the studied samples.

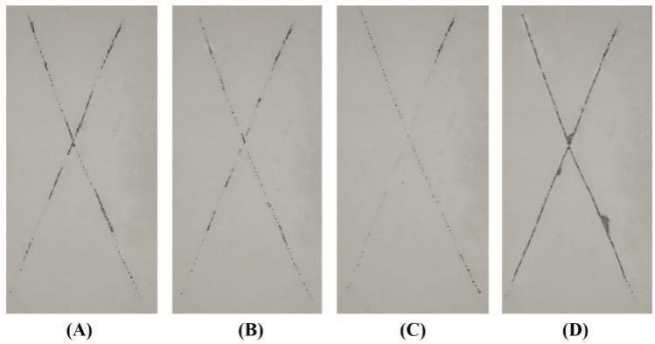

Figure 9. The adhesive tape after it was removed from the studied samples (A) 0 wt.%, (B) 0.42 wt.%, (C) 0.84wt.%, (D) 1.25 wt.%

Table 6. The classification of the adhesion strength of the studied samples

Sample No.	Concentration of Nano-filler SiO_2:CuO, %wt.	Classification of Adhesion Strength
1	0	A3
2	0.42	A4
3	0.84	A4
4	1.25	A3

The increase in adhesion strength when modifying the coating is attributed to the fact that the nanoparticles have a large surface area compared to their size, which means that

introducing these nanoparticles into the coating matrix will increase the contact surface area between the coating layer and the metal substrate surface, which in turn means more frictional force that hinders the separation of the coating layer from the substrate surface, and with increasing the concentration of nanofillers up to 0.84% by weight, the contact surface area between the coating layer and the substrate surface increases and the frictional force increases with it, but after this concentration, the nanoparticles begin to aggregate, which leads on the one hand to reducing their surface area and thus reducing the contact surface area between the coating layer and the substrate surface and also reducing the frictional force, and on the other hand, the agglomeration of nanoparticles leads to deformations in the polymer matrix, which leads to cracks in the coating layer, which reduces the contact surface area between it and the metal substrate, which leads to a decrease in the adhesion strength.

3.10 Comparison of the prepared Nanocoating with a commercial coating

Table 7 provides a comparative overview of the impedance values obtained for the developed SiO_2:CuO nanocoating (0.84 wt%) and a commercially available epoxy-phenolic coating (TK™-34). Initially, both coatings exhibited high impedance values, demonstrating strong corrosion resistance. However, after 72 hours of exposure to a 3.5% sodium chloride solution, the nanocoating retained a higher percentage of its original impedance (approximately 69%) compared to the TK™-34 coating, which exhibited a tenfold decrease. This indicates that the synergy between the SiO_2 and CuO Nanoparticles not only enhances the initial barrier properties but also contributes to extending the product's life under corrosive conditions. The results highlight the ability of the nanoenhanced formulation to compete with, and even outperform, commercial systems in long-term corrosion resistance.

Table 7. Comparison of the prepared nanocoating with a commercial coating

Coating Type	Initial Impedance ($\Omega \cdot cm^2$)	Impedance after 72h ($\Omega \cdot cm^2$)	Impedance Retention (%)
Nano Coating SiO_2:CuO (0.84%)	8.79×10^6	6.10×10^6	69%
Commercial TK™-34 Epoxy Phenolic	1.0×10^7	1.0×10^6	10%

4. DISCUSSION, APPLICATIONS, AND OUTLOOK

The experimental results presented above demonstrated a marked enhancement in the corrosion resistance, adhesion strength, and thermal stability of alkyd coatings upon the incorporation of SiO_2/CuO nanoparticles. Notably, the optimal performance was achieved at a 0.84 wt.% filler concentration with a SiO_2:CuO weight ratio of 0.61:0.39. These findings underscore the critical role of nanoparticle synergy in optimizing coating performance. The following section extends the discussion to industrial implications, economic feasibility, existing limitations, and future research directions.

4.1 Industrial relevance and practical implications

The improved performance of the SiO_2/CuO-modified alkyd coatings indicates strong potential for use in high-risk industrial environments. In marine structures and offshore platforms, where metal degradation is intensified by chloride-induced Corrosion, this coating system offers enhanced barrier protection and thermal stability. Similarly, in chemical processing and water treatment facilities, where corrosion-induced failures can lead to operational shutdowns and environmental hazards, the coating's resilience can significantly reduce maintenance frequency and enhance safety.

The compatibility of the formulation with conventional alkyd coating equipment enables seamless integration into existing industrial coating lines without additional infrastructure investment. Furthermore, the exclusion of toxic corrosion inhibitors positions the coating within the framework of green chemistry, supporting sustainability mandates across infrastructure and industrial sectors.

4.2 Preliminary economic feasibility

The proposed nanocomposite coating exhibits economic advantages due to the low material cost of SiO_2 and CuO nanoparticles and the minimal quantities required for optimal performance. With a peak protective efficiency achieved at only 0.84 wt.%, the additional raw material cost is estimated to remain below 12% per liter of coating. This minor increase is offset by the substantial extension in coating lifespan, projected to exceed 300%, resulting in lower maintenance and recoating demands over time.

Moreover, the high commercial availability and low toxicity of the nanoparticles simplify compliance with environmental and occupational safety regulations. Future cost modeling based on field deployment data can further quantify the return on investment and validate the formulation's economic competitiveness across industries.

4.3 Limitations and future work

The laboratory findings are promising, but certain limitations should be acknowledged. Corrosion testing was conducted under controlled accelerated conditions using a 3.5% NaCl solution, which may not fully replicate the complexities of real-world environments. Furthermore, the study focused exclusively on mild steel substrates, limiting its generalizability to other metals, such as stainless steel or aluminum alloys. The potential for long-term agglomeration of nanoparticles at higher concentrations was not explored, and it may affect performance stability under extended exposure.

Despite hybrid nanofillers such as SiO_2 and CuO offering synergistic anticorrosive benefits, their incorporation presents several technical challenges. Ensuring uniform dispersion within the polymer matrix is complicated by differences in particle size, surface energy, and hydrophilicity. Agglomeration remains a persistent issue at higher filler loadings due to strong van der Waals attractions, which may lead to micro-defects and reduced coating integrity. Moreover, optimizing interfacial interactions between dissimilar nanoparticles and the polymer network requires precise surface functionalization or surfactant selection to avoid phase separation or reduced adhesion. These issues necessitate

advanced dispersion strategies, such as ultrasonication, silane coupling agents, or in-situ polymerization to maintain coating homogeneity and functionality [19, 23].

Future work should include:

I. Long-duration field trials under marine, urban, and industrial conditions.
II. Validation in a broader range of metallic substrates.
III. Exploration of multifunctional additives (e.g., TiO_2, ZnO) for added protective and self-cleaning features.
IV. Development of surface functionalization strategies to improve nanoparticle dispersion at higher loadings.
V. Comprehensive mechanical characterization (abrasion, impact resistance) in conjunction with electrochemical assessments.

4.4 Comparative performance with commercial coatings

A direct comparison between the developed coating and a standard epoxy-phenolic system (TK™-34) revealed the superior durability of the nanocomposite. After 72 hours of salt spray exposure, the SiO_2/CuO coating retained 69% of its initial impedance, compared to a tenfold drop in the commercial reference. This highlights the efficiency of the nanoparticle synergy in maintaining long-term electrochemical protection and affirms the formulation's readiness for competitive industrial deployment.

5. CONCLUSION

This study confirms the efficacy of SiO_2/CuO nanoparticle incorporation in enhancing alkyd-based coating systems. The optimal composition—0.84 wt.% with a SiO_2:CuO ratio of 0.61:0.39—yielded superior corrosion resistance, improved thermal stability, and stronger substrate adhesion. These improvements result from the combined effects of SiO_2's electrical insulation and CuO's hydrophobicity. The coating demonstrated clear advantages over commercial alternatives in both accelerated corrosion testing and adhesion performance. These results support the formulation's potential as a scalable, eco-friendly, and high-performance solution for corrosion protection in demanding industrial environments.

REFERENCES

[1] Mousavi Jarrahi, M., Khajavian, E., Noorbakhsh Nezhad, A.H., Mohammadi Zahrani, E., Alfantazi, A. (2025). Elucidating the electrochemical corrosion of a water pump impeller in an industrial cooling system with zero liquid discharge. Water, 17(2): 173. https://doi.org/10.3390/w17020173

[2] Ravi, K.G., Ramesh, K.V. (2023). Corrosion studies of various salt solutions on metals and alloys. Global Journal of Engineering and Technology Advances, 16(03): 007-018. https://doi.org/10.30574/gjeta.2023.16.3.0174

[3] Dalbouha, A., Rais, Z. (2022). Metal corrosion: In-depth analysis, economic impacts, and inhibition strategies for enhanced infrastructure durability. Journal of Applied Science and Environmental Studies, 5(1): 5-11. https://doi.org/10.48393/IMIST.PRSM/jases-v5i1.45206

[4] Olorundaisi, E., Jamiru, T., Adegbola, A.T. (2020). Mitigating the effect of Corrosion and wear in high strength low alloy steels (HSLA) in the petrochemical transportation industry—a review. Materials Research Express, 6(12). https://doi.org/10.1088/2053-1591/ab65e7

[5] Li, L., Mahmoodian, M., Khaloo, A., Sun, Z. (2021). Risk-cost optimized maintenance strategy for steel bridge subjected to deterioration. Sustainability, 14(1): 436. https://doi.org/10.3390/su14010436

[6] Crawford, K.C. (2023). Perspective chapter: Bridge deterioration and failures. In Structural health monitoring of structure and infrastructure. IntechOpen. https://doi.org/10.5772/intechopen.109927

[7] Rahman, N.A., Ismail, M.C. (2013). Corrosion protection coating for buried pipelines: A short review. International Journal of Material Science Innovations,1(4): 207-2017.

[8] National Association of Corrosion Engineers (NACE). (2022). The global cost of Corrosion. http://impact.nace.org/economic-impact.aspx.

[9] Milošev, I., Scully, J. (2024). AMPP+S: Corrosion protection = sustainability. Materials Performance, 63(12): 1145-1149. https://doi.org/10.5006/4680

[10] Ugural, A.C. (2022). Mechanical Engineering Design (SI Edition). CRC Press. https://doi.org/10.1201/9781003251378

[11] Kaya, O., Gabatel, L., Bellani, S., Barberis, F., Bonaccorso, F., Cole, I., Roche, S. (2024). Advances and challenges of hexagonal boron nitride-based anticorrosion coatings. https://www.researchgate.net/publication/386375451_Advances_and_Challenges_of_Hexagonal_Boron_Nitride-based_Anticorrosion_Coatings.

[12] Taylor, C.D., Tossey, B.M. (2021). High temperature oxidation of corrosion resistant alloys from machine learning. NPJ Materials Degradation, 5(1): 38. https://doi.org/10.1038/s41529-021-00184-3

[13] Xavier, J.R. (2021). Improvement of mechanical and anticorrosion coating properties in poly(propyl methacrylate) with silane functionalized silica nanoparticles. Silicon, 13: 3291-3305. https://doi.org/10.1007/s12633-020-00679-9

[14] Mardare, L., Benea, L. (2021). Effects of TiO_2 nanoparticles on corrosion protection ability of polymeric primer coating system. Polymers, 13(4): 614. https://doi.org/10.3390/polym13040614

[15] Abdel-Karim, A.M., Ahmed, Y.M., El-Masry, M.M. (2023). Ag-CuO/epoxy hybrid nanocomposites as anti-corrosive coatings and self-cleaning on copper substrate. Scientific Reports, 13: 19248. https://doi.org/10.1038/s41598-023-46533-x

[16] Cao, C., Wang, F., Lu, M. (2020). Superhydrophobic CuO coating fabricated on cotton fabric for oil/water separation and photocatalytic degradation. Colloids and Surfaces A: Physicochemical and Engineering Aspects, 601: 125033. https://doi.org/10.1016/j.colsurfa.2020.125033

[17] ASTM International. (2022). Standard test methods for measuring adhesion by tape test (ASTM D3359). https://doi.org/10.1520/D3359-22

[18] Kurdi, A., Tabbakh, T., Alhazmi, H. (2020). Deformation of cold sprayed Ni-Sn coating under micro-pillar compression. Surface and Coatings Technology, 403: 126425.

https://doi.org/10.1016/j.surfcoat.2020.126425
[19] Dias, I.A., Perina, F., Figueiredo, J., Silva, A.RR., Cardoso, D.N., Martins, R. (2025). Sub-lethal effects of innovative anti-corrosion nanoadditives on the marine bivalve Ruditapes philippinarum. Environmental Pollution, 368: 125662.
[20] Nazari, M.H., Zhang, Y., Mahmoodi, A., Xu, G., Yu, J., Wu, J., Shi, X. (2021). Nanocomposite organic coatings for corrosion protection of metals: A review of recent advances. Progress in Organic Coatings, 162: 106573. https://doi.org/10.1016/j.porgcoat.2021.106573
[21] Edvinsson, T. (2018). Optical quantum confinement and photocatalytic properties in two-, one-, and zero-dimensional nanostructures. Royal Society Open Science, 5(9): 180387. https://doi.org/10.1098/rsos.180387
[22] Zaman, M., Poolla, R., Singh, P., Gudipati, T. (2020). Biogenic synthesis of CuO nanoparticles using Tamarindus indica L. and a study of their photocatalytic and antibacterial activity. Environmental Nanotechnology, Monitoring & Management, 14: 100346. https://doi.org/10.1016/j.enmm.2020.100346
[23] Ghaderi, M., Bi, H., Dam-Johansen, K. (2023). Advanced materials for smart protective coatings: Unleashing the potential of metal/covalent organic frameworks, 2D nanomaterials, and carbonaceous structures. Advances in Colloid and Interface Science, 323: 103055. https://doi.org/10.1016/j.cis.2023.103055
[24] Yadav, S., Raman, A.P.S., Singh, M.B., Massey, I., Singh, P., Verma, C., AlFantazi, A. (2024). Green nanoparticles for advanced corrosion protection: Current perspectives and future prospects. Applied Surface Science Advances, 21: 100605. https://doi.org/10.1016/j.apsadv.2024.100605
[25] Swadener, J.G. (2023). Strain engineering of ZrO_2@TiO_2 core@shell nanoparticle photocatalysts. Solar, 3(1): 15-24. https://doi.org/10.3390/solar3010002
[26] Liu, Y., Zhang, Q., Wang, J., Shao, Y., Xu, Z., Wang, Y., Wang, J. (2023). Effect of high-temperature mechanochemistry method modified TiO_2 on the dispersibility and corrosion resistance of TiO_2-epoxy coatings. Anticorrosion Methods and Materials, 70(6): 449-458. https://doi.org/10.1108/ACMM-05-2023-2809
[27] Tavakoli, S., Nemati, S., Kharaziha, M., Akbari-Alavijeh, S. (2019). Embedding CuO nanoparticles in PDMS-SiO2 Coating to improve antibacterial characteristic and corrosion resistance. Colloid and Interface Science Communications, 28: 20-28. https://doi.org/10.1016/J.COLCOM.2018.11.002
[28] Wang, Z., Zhou, X., Shang, Y., Wang, B., Lu, K., Gan, W., Lai, H., Wang, J., Huang, C., Chen, Z., Hao, C., Feng, E., Li, J. (2024). Synthesis and characterization of superhydrophobic epoxy resin coating with SiO_2@CuO/HDTMS for enhanced self-cleaning, photocatalytic, and corrosion-resistant properties. Materials, 17(8): 1849. https://doi.org/10.3390/ma17081849
[29] Yin, H., Liu, H., Guo, X., Cui, Z., Tang, J., Lin, X., Hu, C. (2021). A facile approach to fabricate robust superhydrophobic Cu/TiO_2 composite coating on stainless steel. Vacuum, 195: 110699. https://doi.org/10.1016/j.vacuum.2021.110699
[30] Huang, G., Guo, Y., Lee, B., Chen, H., Mao, A. (2025). Research advances and future perspectives of superhydrophobic coatings in sports equipment applications. Molecules, 30(3): 644. https://doi.org/10.3390/molecules30030644
[31] Mora, L., Taylor, A., Paul, S., Dawson, R, Wang, C., Taleb, W., Owen, J., Neville, A., Barker, R. (2018). Impact of silica nanoparticles on the morphology and mechanical properties of sol-gel derived coatings. Surface & Coatings Technology, 342: 48-56. https://doi.org/10.1016/j.surfcoat.2018.02.080
[32] Ghosh, A., Meyyappan, P., Steele, T.W.J. (2022). Voltage activation of poly(ethylene glycol) diacrylate. Progress in Organic Coatings, 165: 106770. https://doi.org/10.1016/j.porgcoat.2022.106770
[33] Thongjamroon, S., Wootthikanokkhan, J., Poolthong, N. (2023). Photocatalytic performances and antifouling efficacies of alternative marine coatings derived from polymer/metal oxides (WO_3@TiO_2)-based composites. Catalysts, 13(4): 649. https://doi.org/10.3390/catal13040649
[34] Chen, Q., Lei, Y. (2023). Applications of conducting polymers for anticorrosion in marine environments. In Corrosion and protection of marine engineering structures. CRC Press, Taylor & Francis. https://doi.org/10.1201/9781003376194-5
[35] Isacfranklin, M., Daphine, S., Yuvakkumar, R., Kungumadevi, L., Ravi, G., Al-Sehemi, A.G., Velauthapillai, D. (2022). $ZnCo_2O_4$/CNT composite for efficient supercapacitor electrodes. Ceramics International, 48(17): 24745-24750. https://doi.org/10.1016/j.ceramint.2022.05.123
[36] Alqahtani, H.A., AlGhamdi, J.M., Mu'azu, N.D. (2025). Synergistic effects of Zn-rich layered double hydroxides on the corrosion resistance of PVDF-based coatings in marine environments. Polymers, 17(3): 331. https://doi.org/10.3390/polym17030331
[37] Han, Y., Farzaneh, M. (2015). Synthesis and characterization of CeO2-Al2O3 nanocomposite coating on the AA6061 alloy. Advanced Materials Research, 1120-1121: 750-762
[38] Chen, T., Wu, H., Zhang, W., Li, J., Liu, F., Han, E. (2023). A sustainable body-temperature self-healing polyurethane nanocomposite coating with excellent strength and toughness through optimal hydrogen-bonding interactions. Progress in Organic Coatings, 185: 107876. https://doi.org/10.1016/j.porgcoat.2023.107876
[39] Habib, S., Khan, A., Ismail, S.M., Shakoor, R.A., Kahraman, R., Ahmed, E.M. (2023). Polymeric smart coatings containing modified capped halloysite nanotubes for corrosion protection of carbon steel. Journal of Materials Science, 58: 6803-6822. https://doi.org/10.1007/s10853-023-08437-z
[40] Bobeico, E., Mercaldo, L.V., Morvillo, P., Usatii, I., Della Noce, M., Lancellotti, L., Sasso, C., Ricciardi, R., Delli Veneri, P. (2020). Evaporated MoOx as general back-side hole collector for solar cells. Coatings, 10(8): 763. https://doi.org/10.3390/coatings10080763
[41] Suhartini, S., Rohma, N.A., Pratama, A.P.A., Sunyoto, N.M.S., Mardawati, E., Kasbawati, Sulaiman, A.M., Harmayanti, A., Gapsari, F. (2025). Sustainable corrosion protection: Chitosan/reduced graphene oxide nanocomposite coating derived from palm oil empty fruit bunches on low carbon steel. Case Studies in Chemical and Environmental Engineering, 11: 101116. https://doi.org/10.1016/j.cscee.2025.101116

[42] Qureshi, A., Habib, S., Nawaz, M., Shakoor, R.A., Kahraman, R., Ahmed, E.M. (2023). Modified halloysite nanotubes decorated with Ceria for synergistic corrosion inhibition of polyolefin-based smart composite coatings. Applied Clay Science, 234: 106827. https://doi.org/10.1016/j.clay.2023.106827

NOMENCLATURE

SiO_2	Silicon Dioxide
CuO	Copper Oxide
TiO_2	Titanium Dioxide
ZrO_2	Zirconium Dioxide
SEM	Scanning Electron Microscopy
EIS	Electrochemical Impedance Spectroscopy
FTIR	Fourier Transform Infrared Spectroscopy
XRD	X-ray Diffraction
TGA	Thermogravimetric Analysis
ASTM D3359	A standard method for adhesion tape test
PDP	Potentiodynamic Polarization
AISI	American Iron and Steel Institute
NPs	Nanoparticles
TK™-34	Commercial epoxy-phenolic coating
pH	Degree of acidity/basicity
$	Currency symbol (Dollar)

Greek symbols

θ (Theta)	The angle of reflection in XRD measurements
Ω (Omega)	Electrical resistance unit (Ohm)
μm (Micrometer)	Micrometer (small thickness measurement)

Subscripts

cm^2	Area unit (square centimeters) in electrochemical measurements
wt.%	Weight percentage
°C	Degree Celsius for temperature
%	Percentage for concentrations, efficiency, retention